JACS
JOURNAL OF THE AMERICAN CHEMICAL SOCIETY
Cite This: J. Am. Chem. Soc. 2019, 141, 4182−4185
Communication
pubs.acs.org/JACS

Substrate-Driven Transient Self-Assembly and Spontaneous Disassembly Directed by Chemical Reaction with Product Release

Huaxin Wang, Yanyan Wang, Bowen Shen, Xin Liu, and Myongsoo Lee*

State Key Lab of Supramolecular Structure and Materials, College of Chemistry, Jilin University, Changchun 130012, China

Supporting Information

ABSTRACT: The chemical reactivity of molecules can be significantly enhanced when they are trapped in a confined space. Although such a confinement effect can be found in many self-assembled nanostructures, dissipation after completing the reaction to release the product remains elusive. Here we report substrate-directed transient self-assembly for accelerating a chemical reaction and spontaneous disassembly with releasing the products. The hydrophobic substrates mediate self-assembly of a dissolved pyridine-based amphiphile to provide a confined space to promote an aromatic nucleophilic substitution (S_NAr) reaction in water. The chemical reaction triggers disassembly of the aggregates with simultaneous release of the product that can be spontaneously separated out of the solution by precipitation. Neutralization of the amphiphilic molecule leads to a new cycle of self-assembly entrapping substrates and disassembly with releasing the product.

Specific binding of reactants, acceleration of chemical reactions, and then release of products found in enzymatic reactions in nature have become a main source of inspiration for the design of artificial systems with efficient and controlled catalytic activity.[1−3] Similar confinement effects are encountered when substrates are captured within a confined space of self-assembly due to a localization of reacting species within the hydrophobic region of the self-assembly.[4−7] For example, micellar and vesicular aggregates of amphiphilic molecules entrap organic substrates to accelerate the rate of reactions in aqueous environment.[8−11] This entrapment leads to a highly concentrated reaction site that lowers the energy barrier for chemical reactions. Nonetheless, most self-assembled aggregates to accelerate a chemical reaction are based on preformed, fixed structures, thus rendering them incapable of releasing the products into external environments.

To overcome this limitation, one can use a transient formation of self-assembly driven by noncovalent interactions with an additional nonassembling substrate as a chemical fuel.[12−15] The added hydrophobic substrate can effectively stabilize self-assembled aggregates.[16] The substrate entrapped inside the hydrophobic part of the self-assembly would readily convert into products due to space confinement.[9,11] Simultaneously, the conversion of the substrate as the consumption of the fuel would lead to the loss of stabilizing interactions, leading to spontaneous dissociation of the assembly with release of the product. Therefore, the integration of a chemical reaction and an energy consuming process would provide an approach to create the next generation of supramolecular materials with complex functions far beyond what permanent systems can provide. Here we report transient membrane assembly of a pyridine-based amphiphile driven by nonassembling substrates for accelerating a chemical reaction to produce a hydrophobic product and protonic acid. The *in situ* generated protonic acid triggers spontaneous disassembly by protonation of the pyridine-based amphiphile with simultaneous release of the product. After the reaction is completed, a new cycle of self-assembly entrapping substrates and reaction-driven disassembly with releasing the product occurs (Figure 1). The unique feature of this strategy arises from the transient stabilization of membrane assembly driven by additionally added nonassembling substrates, which act as a chemical fuel. The chemical reaction of the substrates leads to spontaneous dissociation of the assembly with releasing the product. The precipitated product can be easily separated from the aqueous solution by filteration.

Amphiphilic molecule **1** that forms the transient self-assembly consists of a pyridine-based aromatic segment and hydrophilic oligoether chains grafted at both the aromatic ends (Figure 1). We hypothesized that the self-assembly of **1** in aqueous solution can provide hydrophobic confined spaces with pyridine environments for an S_NAr reaction to accelerate the reaction rate. When complete conversion of substrates occurs, *in situ* generated HCl leads to the protonation of the pyridine unit of **1**, resulting in disassembly to release the product. In aqueous solution, **1** does not exhibit any noticeable aggregation behavior. In contrast, the addition of hydrophobic thiol reactant **R1** and a stoichiometric amount of an aryl halide into the solution (in a mole ratio **R1**/**1** of 5:1) induces the formation of aggregates due to enhanced hydrophobic interactions, which was confirmed by the decreased intensity of absorption maximum and fluorescence quenching (Figures S6, S7).[16,17] The mutual interaction between **1** and **R1** was also confirmed by FT-IR measurements which show a lower energy shift of the S−H stretching band due to interaction between S−H and pyridine (Figure S9).[18] Upon addition of the substrates, indeed, dynamic light scattering (DLS) experiments revealed a strong scattering peak with a size of ∼200 nm (Figure 2a), which provides further evidence for the formation of aggregates. To visualize the formation of the aggregates, we performed transmission electron microscopy (TEM) experiments upon addition of the reactants into the

Received: November 29, 2018
Published: February 24, 2019

DOI: 10.1021/jacs.8b12777
J. Am. Chem. Soc. 2019, 141, 4182−4185

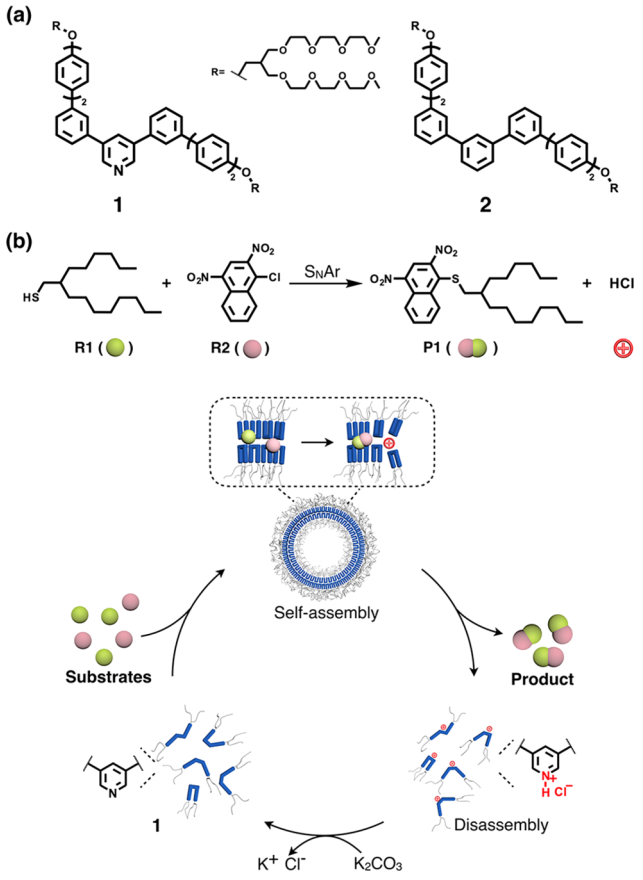

Figure 1. (a) Molecular structure of **1** and **2**. (b) Schematic representation of the substrates-driven transient self-assembly.

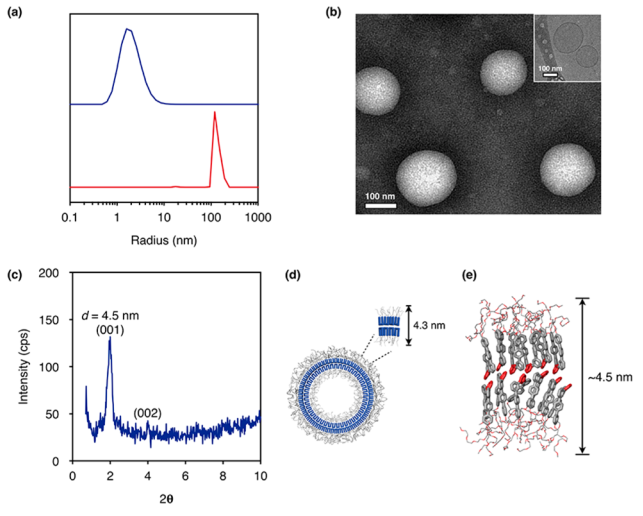

Figure 2. (a) DLS profiles of **1** (75.3 μM) before (blue line) and after (red line) addition of **R1** (mole ratio **R1**/**1** of 5:1) in aqueous solution. (b) Negatively stained TEM image (inset, cryo-TEM image) of **1** (75.3 μM) with addition of **R1** (mole ratio **R1**/**1** of 5:1) in aqueous solution. (c) Powder X-ray diffraction pattern of **1** and **R1** (a mole ratio **R1**/**1** of 5:1) obtained from freeze-dried films of aqueous solution. (d) Schematic representation and (e) molecular simulation of a bilayer membrane structure (red represents pyridine units).

aqueous solution of **1** (Figure 2b). The image shows the formation of vesicular structures. Cryo-TEM investigations confirmed the presence of vesicular aggregates with a dark outer circle with a uniform thickness of 4.3 nm (Figure 2b, inset).[19] The wall thickness was further confirmed by an X-ray diffraction pattern, which showed a layer thickness of 4.5 nm (Figure 2c). This dimension is in good agreement with the expected thickness of a bilayer packing of **1** with a cisoid conformation (Figure 2e). The blue-shifted UV absorption after aggregation is consistent with adopting a cisoid conformation in the aggregation state (Figure S6).[20]

Considering that the vesicular walls consist of a bilayer, the hydrophobic interior would consist of a high density of pyridine units. Accordingly, we envisioned that the hydrophobic pyridine environment of the confined space would function as a nanoreactor for an S_NAr reaction to accelerate (Figure 1). To corroborate the aromatic substitution reaction, we added 1-chloro-2,4-dinitronaphthalene (**R2**) to the aqueous solution of **1** containing **R1** (in a mole ratio **R1**/**1** of 5:1) at room temperature. With time lapse at room temperature, an additional peak corresponding to the reaction product was identified in analytical HPLC of which the intensity increases gradually over 75 min at the expense of **R1** (Figure 3a), demonstrating that the S_NAr reaction of the

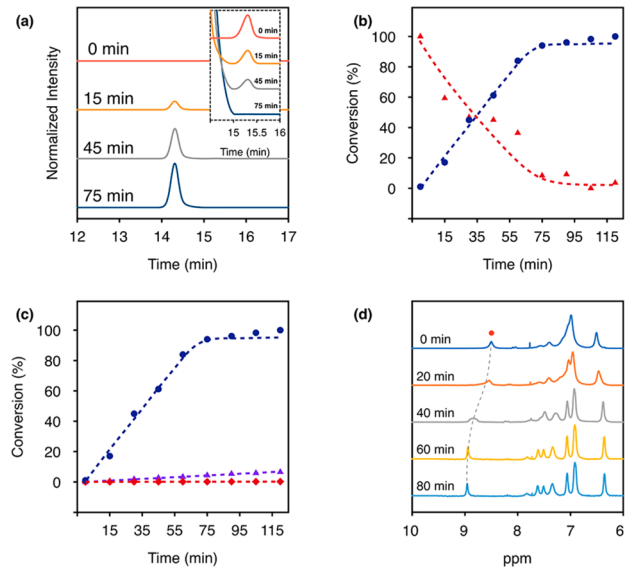

Figure 3. (a) HPLC chromatograms of reaction product (inset: **R1**) with time variation. (b) The conversion (●) and disappearance of **R1** (▲) as a function of time. (c) The conversion of **R1** in the presence of **1** (●), **2** (▲) (75.3 μM, respectively) and without **1** or **2** in $CHCl_3$ (♦). (d) ^{1}H NMR chemical shift for *ortho*-H of pyridine unit (●) of **1** (4.52 mM) with substrates (mole ratio substrates/**1** 3.5:1) in methanol-d_4/D_2O (1:1 v/v) with time variation.

aromatic chloride (**R2**) readily proceeds with the entrapped thiol inside the vesicular walls in water media. The peak intensity levels-off at complete conversion after 75 min (Figure 3b), indicating that the S_NAr reaction of the substrates is completed over 75 min. For a control experiment, we performed the identical S_NAr reaction of **R2** with **R1** in $CHCl_3$ solution in the presence of pyridine in which **1** does not form aggregate structures (Figure 3c). With a lack of aggregation, the reaction did not yield any noticeable product within 2 h. Thus, the self-assembly was able to catalyze the aromatic substitution reaction. The driving force for accelerating the reaction is believed to be the space confinement and the pyridine environment in the hydrophobic

DOI: 10.1021/jacs.8b12777
J. Am. Chem. Soc. 2019, 141, 4182−4185

interior generated by self-assembly.[4,21] The space confinement would considerably increase local concentrations of the two reactants to enhance the reaction rate. Furthermore, the equilibrium between the substrate and products would be shifted toward the product side in a hydrophobic pyridine environment, because *in situ* generated HCl during the reaction would be trapped by the pyridine units. Indeed, ^{1}H NMR measurements showed that the resonance associated with *ortho*-H of the pyridine is downfield shifted as the reaction proceeds (Figure 3d), indicating that the pyridine units entrap *in situ* generated HCl.[22] As a control experiment, we replaced the pyridine unit into a phenylene unit (**2**) in the self-assembling molecule. Although the substrates induce self-assembly (Figure S10), the membrane assembly of **2** does not show an obvious acceleration effect for the S_NAr reaction (Figure 3c), supporting that the hydrophobic pyridine environment in combination with space confinement is a major driving force for the acceleration of the chemical reaction. The acceleration of the reaction rate attributed to the pyridine environment of the hydrophobic inner space was also observed by the thio-etherification with a benzyl bromide (**R3**, Figures S11, S12), demonstrating that our approach to catalyze the reaction is applicable to various types of protonic acid-forming reactions other than S_NAr reaction.

The protonation of the pyridine units by *in situ* generated HCl during the reaction would cause the self-assembled structures to be unstable due to the decreased hydrophobic attraction and mutual electrostatic repulsion in the aromatic interior. Consequently, the membrane structures would be dissociated during conversion of the substrates. Indeed, DLS measurements show that the size of the vesicular aggregates gradually decreases during the chemical reaction (Figure 4b), demonstrating that the conversion of the substrates drives the vesicular membrane assembly to be disintegrated. The TEM images show that, as the chemical reaction undergoes, the vesicles formed in the initial stage gradually collapse into small fragments (Figure 4a). When the reaction is completed after 75 min, TEM and DLS show a lack of any noticeable aggregates (Figure 4b), indicating that the membrane assembly is disintegrated with complete conversion of the substrates. Therefore, the self-assembled membrane structures are transiently stabilized only as far as the substrates exist. The chemical reaction changes the hydrophobic aromatic environment of the membrane interior to be hydrophilic due to entrapping *in situ* generating HCl by the pyridine units, giving rise to spontaneous collapse into the molecular subunits (Figure 4c).

Interestingly, the dissociation of the membrane assembly driven by conversion of the substrates is accompanied by precipitation of the product, indicating that, when protonated, **1** is incapable of self-assembling to capture the hydrophobic product in a water environment. It should be noted that, after complete conversion of the substrates, the hydrophobic product is readily isolated by filtration from the solution without noticeable contamination by **1** (Figure S13). This is because the protonated pyridine unit of **1** becomes highly soluble in water.

Considering that the disassembly originates from the protonation of the pyridine unit, **1** is able to regenerate the self-assembly after neutralization and then addition of the hydrophobic reactants (Figure 1b). Indeed, upon subsequent addition of the substrates into the supernatant solution after removal of the precipitated product by filtration and then

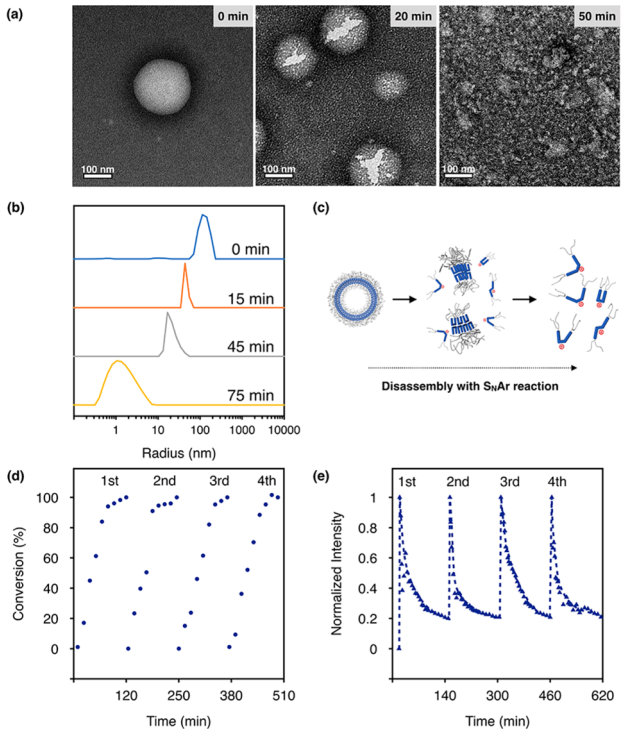

Figure 4. (a) Time-dependent negatively stained TEM images of **1** (75.3 μM) after addition of substrates (mole ratio substrates/**1** of 5:1) in aqueous solution at 0, 20, and 50 min. (b) Time-dependent DLS profiles of **1** (75.3 μM) after addition of substrates (mole ratio reactants/**1** of 5:1) in aqueous solution. (c) Schematic representation of disintegration of membrane assembly with S_NAr reaction. (d) Repeated cycles of HPLC conversions of the reaction as a function of time. (e) Repeated cycles of normalized fluorescence intensity of **1** (75.3 μM) with substrates (mole ratio substrates/**1** of 5:1) in aqueous solution including Nile Red as a probe (mole ratio Nile Red/**1** of 0.5:1) at 560 nm as a function of time. Excitation wavelength: 475 nm.

neutralization with K_2CO_3, a new cycle of assembly with entrapping the reactants and disassembly with releasing products occurs with nearly full conversion over a time scale of 75 min (Figures 4d, S14), which demonstrates that the transient self-assembly can repeatedly accelerate the S_NAr reaction with spontaneous release of the reaction product by disassembly. The repeated cycles of the assembly with entrapping reactants and disassembly with releasing the product were also confirmed by titration experiments using a Nile Red probe (Figure 4e). In the absence of the reactants, the solution of **1** containing Nile Red is not fluorescent at the emission range of Nile Red. Upon the addition of the substrates into the aqueous solution of **1**, however, the fluorescence intensity increases abruptly, indicating that Nile Red is entrapped within the hydrophobic environment of the aggregates.[23] As the reaction proceeds, the enhanced intensity is gradually decayed, indicating that Nile Red becomes exposed to the water environment due to the disassembly of the aggregates. The second reaction cycle is followed by a nearly identical fluorescence enhancement of Nile Red, indicative of the repeated stabilization of the self-assembled membrane structures.

In summary, our results show that substrates can direct transient self-assembly, capable of accelerating chemical reactions by assembly and spontaneous disassembly triggered

DOI: 10.1021/jacs.8b12777
J. Am. Chem. Soc. 2019, 141, 4182−4185

by a chemical reaction, accompanied by releasing the products. After complete conversion of the substrates, the self-assembled membrane structures are dissociated to recover its original disassembled state that is able to undergo a new cycle of self-assembly for accelerating the reaction and disassembly with releasing the product. Such transient behavior will widen opportunities for controlling product formation over versatile chemical transformations in aqueous systems and provide new insight into artificial soft machines regulated by a chemical reaction.

■ ASSOCIATED CONTENT

Supporting Information

The Supporting Information is available free of charge on the ACS Publications website at DOI: 10.1021/jacs.8b12777.

Experimental procedures, synthesis of molecules, NMR data, MALDI-TOF data, spectroscopy data, and TEM images (PDF)

■ AUTHOR INFORMATION

Corresponding Author

*mslee@jlu.edu.cn

ORCID

Myongsoo Lee: 0000-0002-5315-3807

Notes

The authors declare no competing financial interest.

■ ACKNOWLEDGMENTS

This work was supported by the National Natural Science Foundation of China (21634005 and 51473062) and Jilin University Funding (JLUSTIRT).

■ REFERENCES

(1) (a) Küchler, A.; Yoshimoto, M.; Luginbühl, S.; Mavelli, F.; Walde, P. Enzymatic Reactions in Confined Environments. *Nat. Nanotechnol.* **2016**, *11* (5), 409−420. (b) Mitchell, J. B. O. Enzyme Function and Its Evolution. *Curr. Opin. Struct. Biol.* **2017**, *47*, 151−156.

(2) Ichihashi, N.; Yomo, T. Positive Roles of Compartmentalization in Internal Reactions. *Curr. Opin. Chem. Biol.* **2014**, *22*, 12−17.

(3) Tschantz, W. R.; Furfine, E. S.; Casey, P. J. Substrate Binding is Required for Release of Product from Mammalian Protein Farnesyltransferase. *J. Biol. Chem.* **1997**, *272* (15), 9989−9993.

(4) (a) Walde, P.; Umakoshi, H.; Stano, P.; Mavelli, F. Emergent Properties Arising from the Assembly of Amphiphiles. Artificial Vesicle Membranes as Reaction Promoters and Regulators. *Chem. Commun.* **2014**, *50* (71), 10177−10197. (b) Vriezema, D. M.; Comellas Aragonès, M.; Elemans, J. A. A. W.; Cornelissen, J. J. L. M.; Rowan, A. E.; Nolte, R. J. M. Self-Assembled Nanoreactors. *Chem. Rev.* **2005**, *105* (4), 1445−1489.

(5) Gruber, B.; König, B. Self-Assembled Vesicles with Functionalized Membranes. *Chem. - Eur. J.* **2013**, *19* (2), 438−448.

(6) Peters, R. J. R. W.; Louzao, I.; van Hest, J. C. M. From Polymeric Nanoreactors to Artificial Organelles. *Chem. Sci.* **2012**, *3* (2), 335−342.

(7) Maiti, S.; Fortunati, I.; Ferrante, C.; Scrimin, P.; Prins, L. J. Dissipative Self-Assembly of Vesicular Nanoreactors. *Nat. Chem.* **2016**, *8* (7), 725−731.

(8) Dwars, T.; Paetzold, E.; Oehme, G. Reactions in Micellar Systems. *Angew. Chem., Int. Ed.* **2005**, *44* (44), 7174−7199.

(9) Grochmal, A.; Prout, L.; Makin-Taylor, R.; Prohens, R.; Tomas, S. Modulation of Reactivity in the Cavity of Liposomes Promotes the Formation of Peptide Bonds. *J. Am. Chem. Soc.* **2015**, *137* (38), 12269−12275.

(10) Kim, Y.; Kang, J.; Shen, B.; Wang, Y.; He, Y.; Lee, M. Open-Closed Switching of Synthetic Tubular Pores. *Nat. Commun.* **2015**, *6* (1), 8650.

(11) Lee, M.; Jang, C.-J.; Ryu, J.-H. Supramolecular Reactor from Self-Assembly of Rod-Coil molecule in Aqueous Environment. *J. Am. Chem. Soc.* **2004**, *126* (26), 8082−8083.

(12) (a) Fanlo-Virgós, H.; Alba, A.-N. R.; Hamieh, S.; Colomb-Delsuc, M.; Otto, S. Transient Substrate-Induced Catalyst Formation in a Dynamic Molecular Network. *Angew. Chem., Int. Ed.* **2014**, *53* (42), 11346−11350. (b) van Rossum, S. A. P.; Tena-Solsona, M.; van Esch, J. H.; Eelkema, R.; Boekhoven, J. Dissipative Out-of-Equilibrium Assembly of Man-Made Supramolecular Materials. *Chem. Soc. Rev.* **2017**, *46* (18), 5519−5535. (c) van Ravensteijn, B. G. P.; Hendriksen, W. E.; Eelkema, R.; van Esch, J. H.; Kegel, W. K. Fuel-Mediated Transient Clustering of Colloidal Building Blocks. *J. Am. Chem. Soc.* **2017**, *139* (29), 9763−9766.

(13) Zhao, H.; Sen, S.; Udayabhaskararao, T.; Sawczyk, M.; Kučanda, K.; Manna, D.; Kundu, P. K.; Lee, J.-W.; Král, P.; Klajn, R. Reversible Trapping and Reaction Acceleration within Dynamically Self-Assembling Nanoflasks. *Nat. Nanotechnol.* **2016**, *11* (1), 82−88.

(14) Boekhoven, J.; Hendriksen, W. E.; Koper, G. J. M.; Eelkema, R.; van Esch, J. H. Transient Assembly of Active Materials Fueled by a Chemical Reaction. *Science* **2015**, *349* (6252), 1075−1079.

(15) Wojciechowski, J. P.; Martin, A. D.; Thordarson, P. Kinetically Controlled Lifetimes in Redox-Responsive Transient Supramolecular Hydrogels. *J. Am. Chem. Soc.* **2018**, *140* (8), 2869−2874.

(16) Kim, H.-J.; Kim, T.; Lee, M. Responsive Nanostructures from Aqueous Assembly of Rigid-Flexible Block Molecules. *Acc. Chem. Res.* **2011**, *44*, 72−82.

(17) (a) Görl, D.; Zhang, X.; Würthner, F. Molecular Assemblies of Perylene Bisimide Dyes in Water. *Angew. Chem., Int. Ed.* **2012**, *51* (26), 6328−6348. (b) Shin, S.; Lim, S.; Kim, Y.; Kim, T.; Choi, T.-L.; Lee, M. Supramolecular Switching between Flat Sheets and Helical Tubules Triggered by Coordination Interaction. *J. Am. Chem. Soc.* **2013**, *135* (6), 2156−2159.

(18) Mielcarek, A.; Dołęga, A. Weak Hydrogen Bonding Interaction S−H···O = C Studied by FT-IR Spectroscopy and DFT Calculations. *J. Mol. Struct.* **2016**, *1103*, 217−223.

(19) Chen, X.; He, Y.; Kim, Y.; Lee, M. Reversible, Short α-Peptide Assembly for Controlled Capture and Selective Release of Enantiomers. *J. Am. Chem. Soc.* **2016**, *138* (18), 5773−5776.

(20) Kim, H.-J.; Zin, W.-C.; Lee, M. Anion-Directed Self-Assembly of Coordination Polymer into Tunable Secondary Structure. *J. Am. Chem. Soc.* **2004**, *126* (22), 7009−7014.

(21) Murakami, Y.; Kikuchi, J.-i.; Hisaeda, Y.; Hayashida, O. Artificial Enzymes. *Chem. Rev.* **1996**, *96* (2), 721−758.

(22) Roy, G.; Miravet, J. F.; Escuder, B.; Sanchez, C.; Llusar, M. Morphology Templating of Nanofibrous Silica through pH-Sensitive Gels: "*In Situ*" and "Post-Diffusion" Strategies. *J. Mater. Chem.* **2006**, *16*, 1817−1824.

(23) Sackett, D. L.; Wolff, J. Nile Red as a Polarity-Sensitive Fluorescent Probe of Hydrophobic Protein Surfaces. *Anal. Biochem.* **1987**, *167* (2), 228−234.

DOI: 10.1021/jacs.8b12777
J. Am. Chem. Soc. 2019, 141, 4182−4185